# NASA

# MEMORANDUM

EXPERIMENTAL PERFORMANCE OF GASEOUS HYDROGEN AND

LIQUID OXYGEN IN UNCOOLED 20,000-POUND-

THRUST ROCKET ENGINES

By Edward A. Rothenberg, Franklin J. Kutina, Jr., and
George R. Kinney

Lewis Research Center
Cleveland, Ohio

# NATIONAL AERONAUTICS AND SPACE ADMINISTRATION
## WASHINGTON
March 1959

NATIONAL AERONAUTICS AND SPACE ADMINISTRATION

MEMORANDUM 4-8-59E

EXPERIMENTAL PERFORMANCE OF GASEOUS HYDROGEN AND LIQUID OXYGEN

IN UNCOOLED 20,000-POUND-THRUST ROCKET ENGINES*

By Edward A. Rothenberg, Franklin J. Kutina, Jr., and

George R. Kinney

SUMMARY

Experiments were conducted with gaseous hydrogen and liquid oxygen in uncooled rocket chambers of 20,000-pound thrust at a chamber pressure of 300 pounds per square inch absolute. A showerhead injector was used. Data were obtained with from 11 to 24 percent hydrogen in the propellant and with three combustion-chamber lengths. Specific impulse ranged from 94 to 98 percent of theoretical for equilibrium expansion, highest values occurring at the highest percent fuel mixtures. Maximum specific impulse was 350 pound-seconds per pound at 23.5 percent hydrogen. Performance was unaffected by changes in combustion-chamber length which varied the distance from the injector to the throat from 17.8 to 7.8 inches.

INTRODUCTION

The hydrogen-oxygen propellant combination offers very high specific impulse. The maximum theoretical performance is within 5 percent of that of the hydrogen-fluorine combination, which is the highest obtainable with any stable chemical propellants. The experimental performance and operating characteristics described in this report for gaseous hydrogen with liquid oxygen were determined as a preparatory step for investigations with liquid hydrogen in regeneratively cooled engines.

Hydrogen has unique physical properties which make it desirable as a rocket fuel. Its low viscosity, high specific heat, and low critical pressure make it an excellent regenerative coolant. Hydrogen enters the combustion chamber above its low critical temperature after cooling the thrust chamber. This gives the advantage of achieving complete combustion in a smaller chamber, since time is not required for vaporization of the fuel.

---

*Title, Unclassified.

One disadvantage is the low boiling point of hydrogen. Also, its low density produces a significantly lower over-all density than most other propellants; about one-quarter of the propellant weight must be hydrogen if maximum specific impulse is achieved with oxygen. A low density results in larger tanks and greater structural weight in a missile.

When used with oxygen, hydrogen offers a combination in which neither the propellants nor the exhaust products are toxic or corrosive. Therefore, the handling and firing problems are greatly simplified.

Small-scale engine tests (100- to 500-lb thrust) have been made (refs. 1 and 2) to investigate performance and regenerative cooling with the hydrogen-oxygen combination. Work has also been done at 400- and 3000-pound thrust (refs. 3 and 4). In addition, a study of injection fundamentals with hydrogen and oxygen at 200-pound thrust was made (ref. 5). Engine experiments at thrusts greater than 3000 pounds are lacking.

The following were investigated at 20,000-pound thrust at a chamber pressure of 300 pounds per square inch absolute:

(1) Experimental performance potential

(2) Space required for complete combustion

(3) Effect of percent hydrogen in the propellant on performance parameters

(4) Engine operating characteristics such as combustion stability

Gaseous hydrogen, at ambient temperature, was used rather than liquid hydrogen because the engines were not regeneratively cooled. With cooled engines the hydrogen entering the injector would be considerably above its critical temperature. The injector used was a showerhead type. Uncooled steel thrust chambers with refractory coatings were used. Runs were made with from 11 to 24 percent hydrogen in the propellant. Experimental specific impulse, characteristic velocity, and thrust coefficient are shown as functions of percent fuel for three combustion-chamber lengths.

EQUIPMENT AND PROCEDURE

Facility

Figure 1 shows three of the four main parts of the facility. In the center is the test building, which houses the engine test stand, high-pressure propellant tanks and piping, and service areas. The stack

A few test runs were made in air at a Mach number of 6.9 in an attempt to correlate data on flutter models tested in two mediums.

## SYMBOLS

| | |
|---|---|
| $a$ | free-stream speed of sound, ft/sec |
| $b$ | semichord, in. |
| $C_p$ | pressure coefficient |
| $c$ | chord, in. |
| $d$ | shaft width, in. |
| $f$ | frequency, cps |
| $I_\alpha$ | mass moment of inertia about the elastic axis per unit length, $\text{slug-ft}^2/\text{ft}$ |
| $M$ | Mach number |
| $m$ | mass per unit length, slugs/ft |
| $p_o$ | stagnation pressure, lb/sq ft |
| $q$ | dynamic pressure, lb/sq ft |
| $R$ | $\dfrac{b\omega_\alpha}{a}\sqrt{\mu}$, a stiffness-altitude parameter |
| $S_\alpha$ | static unbalance about the elastic axis per unit length, positive for center of gravity back of elastic axis, slug-ft/ft |
| $t$ | shaft thickness, in. |
| $U$ | free-stream velocity, ft/sec |
| $w$ | downwash velocity, ft/sec |
| $x_o$ | elastic-axis position in fraction of the chord, measured from the leading edge |

| | |
|---|---|
| μ | mass of model divided by mass of fluid contained in a cylinder determined by the model, $m/\pi\rho b^2$ |
| ρ | density of test medium, slugs/cu ft |
| τ | maximum thickness of model in fraction of the chord |
| ω | circular frequency, radians/sec |

Subscripts:

| | |
|---|---|
| c | calculated quantity |
| e | experimentally determined quantity |
| f | quantity at flutter |
| h | bending mode |
| α | torsion mode |
| ∞ | free-stream conditions |

## APPARATUS

### Langley Hypersonic Aeroelasticity Tunnel

Most of the tests were performed in the Langley hypersonic aeroelasticity tunnel which uses helium as a test medium. A sketch of this blowdown tunnel is shown in figure 1. The nozzle used in the tests has circular cross sections with a 1.41-inch-diameter minimum section and an 8-inch-diameter test section. Helium is supplied to the stagnation chamber at pressures up to 1,200 pounds per square inch from which dynamic pressures of over 5,000 pounds per square foot are obtainable. The downstream end of the tunnel is connected to a vacuum chamber which can be operated at pressures as low as 1/2 inch of mercury absolute. Stagnation temperature is essentially constant during a run and corresponds to atmospheric temperature. With the available high-pressure helium supply, test runs are of approximately 30-second duration.

Models are wall-mounted on a removable plate which is contoured to maintain a circular test section. The opposite wall is made of transparent plastic; thus, the model could be observed during the test runs. Mach number surveys have been made across the diameter of the tunnel at

from 50 to 100 feet. The water used in the silencer leaves through a drain and was collected in a 130,000-gallon detention tank before being pumped into the sewer system. Both the exhaust duct and the detention tank were designed as pressure vessels for 300 pounds per square inch to withstand possible detonations.

## Engines

Thrust chamber. - The uncooled chambers used for all tests are illustrated in figure 5. The three different chamber configurations used in the tests are listed in the table in figure 5. Only two dimensions were varied, the chamber length (injector to throat) and the divergence angle. The chambers were designed for 20,000-pound thrust with sea-level expansion at a chamber pressure of 300 pounds per square inch absolute. The contraction area ratio was 1.9 and the expansion area ratio 3.68. The chambers were constructed of 1/2-inch-thick carbon steel except for the heavier throat section. The inner surface of the thrust chamber was coated with an aluminum oxide refractory.

Propellant injectors. - The injector was a showerhead type with axial jets for hydrogen and oxygen. A cutaway view of the injector is shown in figure 6. It was constructed of stainless steel with a fuel-cooled copper face plate.

The fuel entered the injector around its periphery from a separate distribution manifold (not shown in fig. 6). After cooling the face plate (as drawn in fig. 6), it was injected into the chamber through 1160 holes, 0.067 inch in diameter. Hydrogen injection velocities for these tests ranged from 2000 to 3500 feet per second and injector pressure drop from 50 to 250 pounds per square inch. The oxidant entered the injector at the back and was carried through the fuel passage in 553 copper tubes. Each tube supplied a 0.043-inch injection hole. The pressure drop across the oxidant orifices ranged from 130 to 300 pounds per square inch.

The fuel and oxidant holes were uniformly and symmetrically spaced except around the periphery; only fuel was injected through the outermost holes. The injection pattern can be seen in the photograph of the injector in figure 7. This same injector was modified for one series of tests. The modification consisted merely of blocking the 64 outermost oxidant holes.

## Instrumentation

Thrust. - Thrust was measured with strain-gage load cells. Three units in the form of Morehouse rings were fastened at 120° intervals to

a ring at the base on the thrust stand. The outputs of the cells were summed electrically and recorded on a self-balancing potentiometer. Thrust calibrations were performed by applying force to the thrust stand with pneumatic jacks located adjacent to load cells. Extensive calibrations under various conditions of use indicated that the probable error in thrust measurement was 0.6 percent.

Pressures. - Chamber pressure, propellant injection pressures, fuel-line pressure at the flowmeter, and propellant flowmeter pressure drops were all measured with strain-gage pressure transducers. The output of each of the transducers was recorded on both self-balancing potentiometers and a direct-reading oscillograph. Each pressure transducer was calibrated prior to each operation. The probable error of the pressure measurements, as recorded on the potentiometers, was no greater than 0.75 percent.

Flow rates. - Oxidant flow was measured with a Venturi flowmeter, calibrated in the flow system with liquid oxygen. The calibration standard was the total weight of oxygen used. Large quantities of oxygen were used at steady flow for each point so that the error in weight measurement produced a small error in flow-rate determination. The fuel flow was metered through an orifice plate machined to ASME standards. The probable error in flow measurements, including density determinations, was less than 1.25 percent.

Temperatures. - Oxidant flowmeter and injection temperatures were measured with copper-constantan thermocouples. Liquid nitrogen was used as a reference temperature. Bare-junction iron-constantan thermocouples were used to measure fuel temperatures at the flowmeter and injector. A reference temperature of 150° F, maintained by an oven, was used for the fuel thermocouples. All temperatures were recorded on self-balancing potentiometers.

Test Procedure

Initial firings indicated that data could be obtained with runs of 3- to 4-second duration. Starting transients lasted about 1.5 seconds, leaving at least 1.5 seconds of steady conditions. This time was more than sufficient for the fast-response instrumentation to provide accurate data. The engine was examined between firings in order to exclude data from any damaged engine.

Firing procedure. - Engine firing was controlled by means of an electrical sequence timer. This timer programmed both the start and shutdown of the engine as well as operation of exhaust-duct-water and carbon-dioxide valves, the instrument chart drives, safety controls, and so forth.

Two engine starting procedures were used. Both procedures resulted in the engine being brought up to full thrust in about 1 second. The first system was a staged start, using about one-third of full running flows as the low-flow stage. Propellants were ignited by an external propane-oxygen torch. When they were burning properly, the engine was brought up to full thrust. A pressure-limiting switch was ·then used to prevent engine operation below a preset chamber pressure. The second system eliminated the staging operation. Both propellant flows were increased uniformly from no flow to full running flows in about 1 second. Ignition took place during this increase. Again, chamber pressure was monitored to ensure proper operation of the engine. No difficulty was experienced with either of the starting systems.

Safety. - The use of gaseous hydrogen as a propellant requires a greater number of safety precautions than use of hydrocarbons. Hazards stem from the extremely wide explosive and flammability limits of hydrogen. All lines which carried high-pressure hydrogen were first carefully purged with low-pressure gas to ensure that air or oxygen would not be compressed with the hydrogen. All vented hydrogen was released 40 feet above the ground in order to aid the dispersion of the gas. The vent stack was continually inerted with carbon dioxide. A gas sampling system was used to detect any hydrogen leaks.

Since most of the runs were fuel-rich, hydrogen accumulated in the exhaust duct. About 3 tons of carbon dioxide were added to the duct prior to firing to lower the oxygen content and hence reduce the explosive hazard. Additional carbon dioxide was added during the shutdown to make up for that swept from the duct by the exhaust gases. The oxygen content of the duct was continually sampled to ensure that an adequately inert atmosphere was maintained.

RESULTS AND DISCUSSION

Performance

Performance data obtained with hydrogen and oxygen are presented in figure 8. Figure 8(a) shows specific impulse as a function of weight percent hydrogen in the propellant. The dotted curve is the theoretical specific impulse calculated for equilibrium expansion, a hydrogen injection temperature of $500^{\circ}$ R, and an axial exhaust. A curve based on frozen-composition expansion is also included for comparison. The solid curve shows the performance obtained with a showerhead injector in engines from 7.8 to 17.8 inches long. There is no discernible difference in performance among the various engine lengths. Specific impulse varied from 291 pound-seconds per pound (94 percent of theoretical) at

11 percent fuel to 350 pound-seconds per pound (98 percent of theoretical) at 23.5 percent fuel. The ratio of the experimental data to the theoretical is illustrated graphically in figure 8(b).

No corrections were made to the data for either exhaust-nozzle divergence or thermodynamic unavailability due to the low contraction ratio. These corrections would total almost 2 percent for the conditions of testing. It would appear then that the specific impulse obtained in the region of peak theoretical performance (approx. 23 to 25 percent fuel) is very near the maximum theoretically obtainable. With less fuel, however, performance dropped off with respect to theoretical; the decrease was several percent in the stoichiometric region.

Data obtained with the showerhead injector modified by blocking the outer ring of oxidant holes are included in figure 8(a). The modification resulted in a significant drop in performance in the shortest engine. Specific impulse varied from 276 pound-seconds per pound (86.5 percent of theoretical) at 12 percent fuel to 336 pound-seconds per pound (94 percent of theoretical) at 22 percent fuel. These data indicate that maldistribution of propellants can reduce performance substantially. This is particularly true in the stoichiometric region where all the hydrogen is needed to combine with the oxygen.

Figure 9 shows characteristic velocity and thrust coefficient as functions of weight percent hydrogen. A calculated pressure was used to establish values for characteristic velocity and thrust coefficient. This calculation, which is discussed in reference 6, was based on a pressure measured in the chamber at the injector and took into account the nonisentropic acceleration of the gases through the chamber and the high injection momentum of the fuel. This calculated chamber pressure was as much as 3 percent lower than the measured pressure, the difference increasing with decreasing percent fuel.

The values of characteristic velocity were within a few percent of the theoretical for all chamber lengths. The trends indicated by these data are in agreement with those established by the specific-impulse data, including the decrease in performance with the modified injector. The thrust-coefficient data (94 to 97.5 percent of theoretical) show lowest values with respect to theoretical in the stoichiometric region, but the differences involved are small. The calculated values presented for thrust coefficient and characteristic velocity are not considered accurate enough to distinguish performance effects within a few percent. A summary of the data obtained is presented in table I. It should be noted that the chamber pressure tabulated is the measured injector end pressure, while the values of characteristic velocity and thrust coefficient are based on the calculated pressures.

Calculations were made of the length of chamber required to achieve essentially complete combustion for these experiments. The calculations were based on the methods described in references 7 and 8. Vaporization of the least volatile propellant, in this case the oxidant, was assumed the controlling parameter in determining the combustion efficiency. An approximate model describing the injector atomization and the chamber gas conditions was used in calculating the length required to vaporize the oxidant. These computations indicated that high combustion efficiencies (97 to 100 percent) should be expected with the chamber lengths used in these experiments (17.8 to 7.8 in.) with a small reduction for the shortest length.

## Operating Characteristics

No evidence of combustion oscillation was found during the testing. There were no indications of injector face burning during this program. The bulk of the cooling load was assigned to hydrogen, which was directed uniformly at high velocity across the entire injector face with the exception of the oxidant orifices. The high-conductivity copper face tended to prevent local overheating. In addition, the showerhead injector type would tend to minimize face heating due to recirculation turbulence.

In general, the uncooled engines showed good durability. However, the shortest engine burned through very quickly in the convergent section of the nozzle with the unmodified injector. In this case, the outermost oxidant jets aimed directly at the convergent section, which began only 1 inch from the injector face. The injector was modified, by plugging of the outermost oxidant holes, to avoid burnout. This had the effect of removing oxygen, and combustion, from the wall and provided a relatively cool hydrogen-rich atmosphere. The short engine (7.8 in.) operated with this modified injector over the range of mixture ratios from stoichiometric to peak performance without damage. However, performance decreased as noted previously. The photograph in figure 10 shows the effect on the combustion chambers of operation with the showerhead and modified showerhead injectors.

With the longer chambers, burned streaks usually developed after several runs. The streaks corresponded to the regions on the injector where the oxidant holes were closest to the chamber wall. These streaks did not hamper operations, but provided further evidence that improvements in propellant injection near the walls could be made. None of the engine burning was considered to be a result of combustion instability. Sound recordings made through a microphone located adjacent to the engine did not produce any audible combustion oscillations.

## SUMMARY OF RESULTS

Experiments were conducted with gaseous hydrogen and liquid oxygen in 20,000-pound-thrust uncooled engines at a chamber pressure of 300 pounds per square inch absolute. Data were obtained with from 11 to 24 percent hydrogen in the propellant and with three combustion-chamber lengths. The injector was a showerhead type. The results were as follows:

1. Specific impulse ranged from 94 to 98 percent of theoretical for equilibrium expansion. The highest percentages of theoretical were at the highest percent fuel mixtures. The maximum value was 350 pound-seconds per pound at 23.5 percent fuel.

2. Values of characteristic velocity were all within a few percent of theoretical.

3. Thrust coefficient varied from 94 to 97.5 percent of theoretical equilibrium expansion.

4. Performance was unaffected by varying the distance from injector to throat from 17.8 to 7.8 inches.

5. No combustion oscillations occurred.

6. There was no burning of the injector face.

Lewis Research Center
National Aeronautics and Space Administration
Cleveland, Ohio, January 9, 1959

## REFERENCES

1. Johnston, Herrick L., and Doyle, William L.: Development of the Liquid Hydrogen-Liquid Oxygen Propellant Combination for Rocket Motors. Tech. Rep. No. 7, Res. Foundation, The Ohio State Univ., Dec. 1951.

2. Baker, Dwight J.: Regenerative Cooling Tests of Rocket Motors Using Liquid Hydrogen and Liquid Oxygen. Rep. No. 4-53, Jet Prop. Lab., C.I.T., Aug. 11, 1949. (Contract W-04-200-ORD-455.)

3. Young, D. A.: Research and Development of Hydrogen-Oxygen Rocket Engine, Model XLR 16-AJ-2. Rep. 378, Jan. 1, Mar. 31, 1949, Aero-jet Eng. Corp., May 11, 1949. (Contract NOa(s) 8496.)

E-218

4. Young, D. A.:  Research and Development of Hydrogen-Oxygen Rocket
      Engine, Model XLR-AJ-2.  Rep. 397, Aerojet Eng. Corp., Sept. 28,
      1949.  (Contract NOa(s) 8496.)

5. Auble, Carmon M.:  A Study of Injection Processes for Liquid Oxygen
      and Gaseous Hydrogen in a 200-Pound-Thrust Rocket Engine.  NACA
      RM E56I25a, 1956.

6. Huff, Vearl N., Fortini, Anthony, and Gordon, Sanford:  Theoretical
      Performance of JP-4 Fuel and Liquid Oxygen as a Rocket Propellant.
      II - Equilibrium Composition.  NACA RM E56D23, 1956.

7. Priem, Richard J.:  Propellant Vaporization as a Criterion for Rocket
      Engine Design; Calculations Using Various Log-Probability Distribu-
      tions of Heptane Drops.  NACA TN 4098, 1957.

8. Heidmann, Marcus F., and Priem, Richard J.:  Propellant Vaporization
      as a Criterion for Rocket Engine Design; Relation Between Percentage
      of Propellant Vaporized and Engine Performance.  NACA TN 4219, 1958.

E-218

CC-2 back

E-218

TABLE I. - EXPERIMENTAL DATA

| Engine chamber length, in. | Oxidant flow, lb/sec | Fuel flow, lb/sec | Percent fuel | Fuel injector pressure, lb/sq in. abs | Chamber pressure (measured), lb/sq in. abs | Specific impulse, lb-sec/lb | Characteristic velocity (corrected), ft/sec | Thrust coefficient (corrected) |
|---|---|---|---|---|---|---|---|---|
| 17.8 | 44.5 | 13.2 | 22.6 | 565 | 315 | 345 | 8340 | 1.331 |
| | 48.2 | 13.7 | 22.2 | 594 | 345 | 354 | 8470 | 1.344 |
| | 48.3 | 11.6 | 19.4 | 510 | 322 | 341 | 8110 | 1.353 |
| | 55.5 | 12.1 | 18.0 | 574 | 359 | 346 | 7980 | 1.395 |
| | 51.6 | 9.8 | 16.0 | 448 | 320 | 328 | 7800 | 1.355 |
| | 52.4 | 8.7 | 14.2 | 397 | 303 | 313 | 7410 | 1.361 |
| | 54.4 | 8.5 | 13.5 | 397 | 311 | 310 | 7370 | 1.355 |
| | 55.9 | 7.1 | 11.3 | 348 | 300 | 294 | 7070 | 1.337 |
| 11.8 | 42.9 | 13.2 | 23.6 | 569 | 306 | 355 | 8280 | 1.378 |
| | 48.0 | 11.2 | 18.9 | 490 | 310 | 336 | 7830 | 1.380 |
| | 51.9 | 9.9 | 16.0 | 453 | 314 | 326 | 7570 | 1.384 |
| | 59.7 | 7.7 | 11.4 | 377 | 310 | 291 | 6780 | 1.381 |
| 7.8 | 45.1 | 13.0 | 22.3 | 572 | 321 | 343 | 8290 | 1.329 |
| | 49.9 | 11.4 | 18.6 | 509 | 332 | 337 | 8050 | 1.346 |
| | 60.5 | 7.6 | 11.1 | 392 | 328 | 296 | 7070 | 1.347 |
| a7.8 | 46.3 | 13.1 | 22.0 | 560 | 315 | 336 | 8080 | 1.337 |
| | 49.9 | 10.7 | 17.7 | 467 | 308 | 324 | 7650 | 1.361 |
| | 59.4 | 8.5 | 12.5 | 404 | 302 | 277 | 6650 | 1.335 |
| | 60.7 | 8.0 | 11.7 | 396 | 308 | 276 | 6680 | 1.335 |

aModified injector used.

E-218

C-45924



Figure 1. - Rocket engine research facility for high-energy propellants.
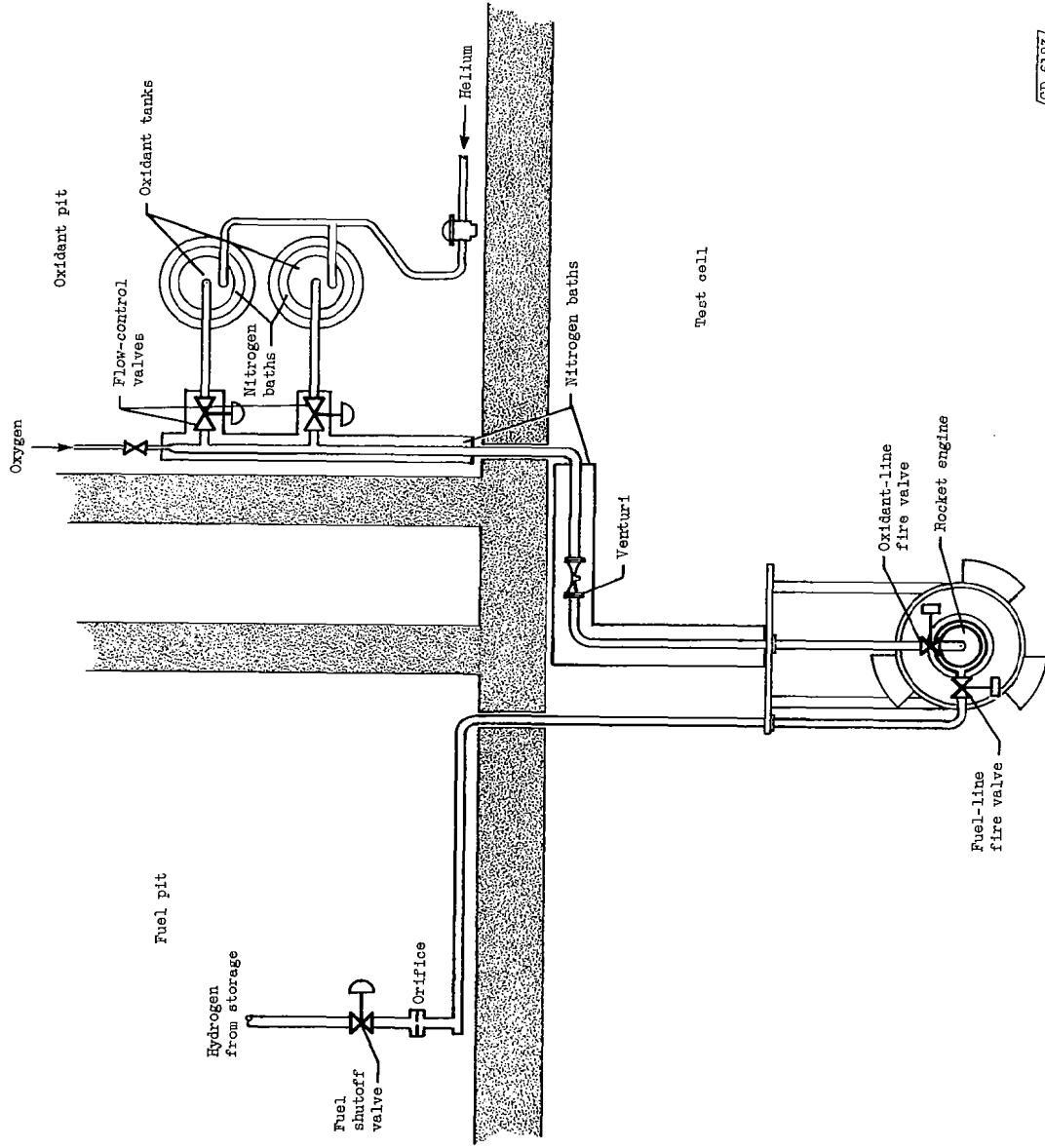
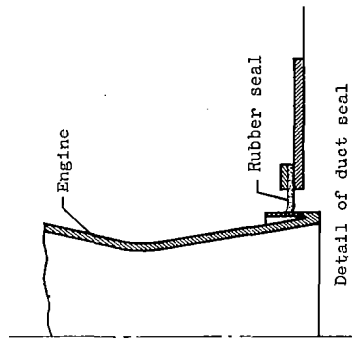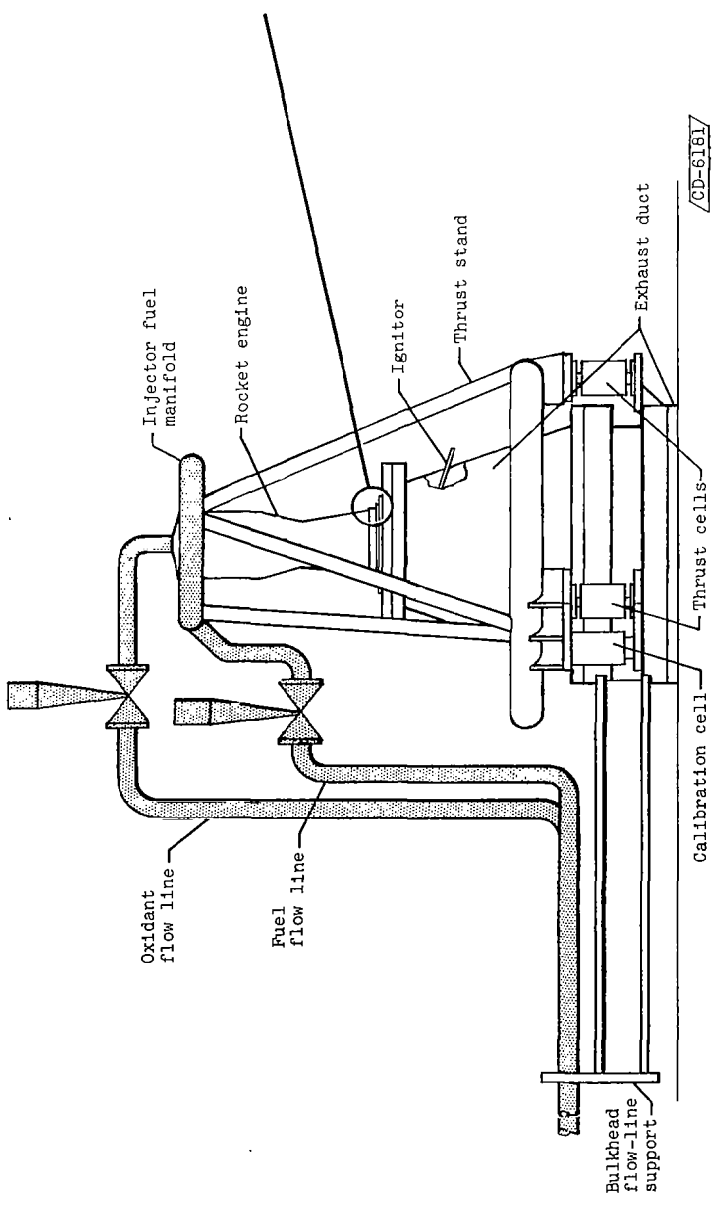Figure 2. - Arrangement of propellant systems in test building.

CD-6183

E-218

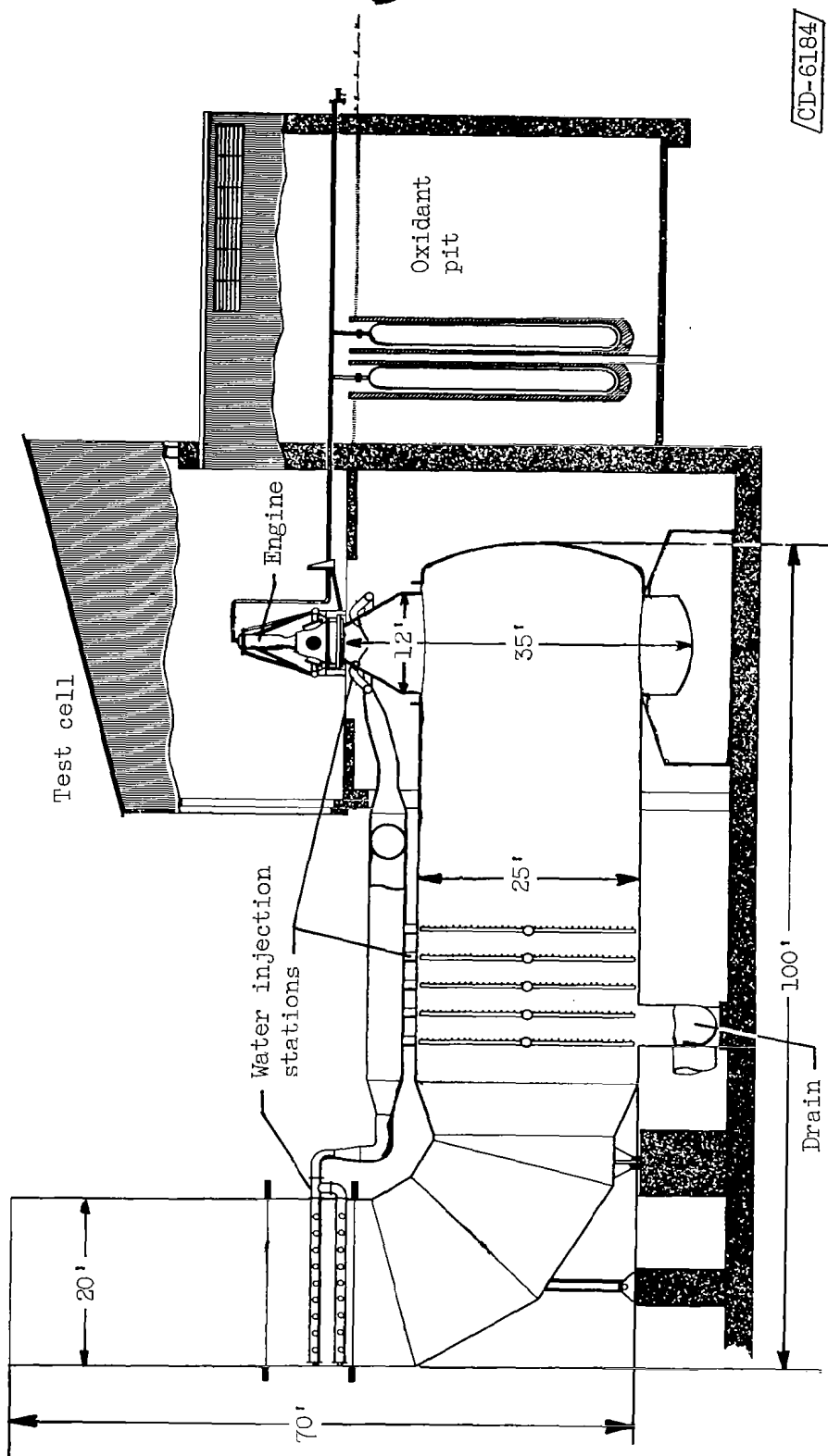E-218



Figure 3. - Diagram of engine on thrust stand.

Oxidant pit

Engine

Test cell

12'

35'

25'

Water injection stations

100'

Drain

20'

70'

CD-6184

Figure 4. - Cross-sectional view of exhaust duct.
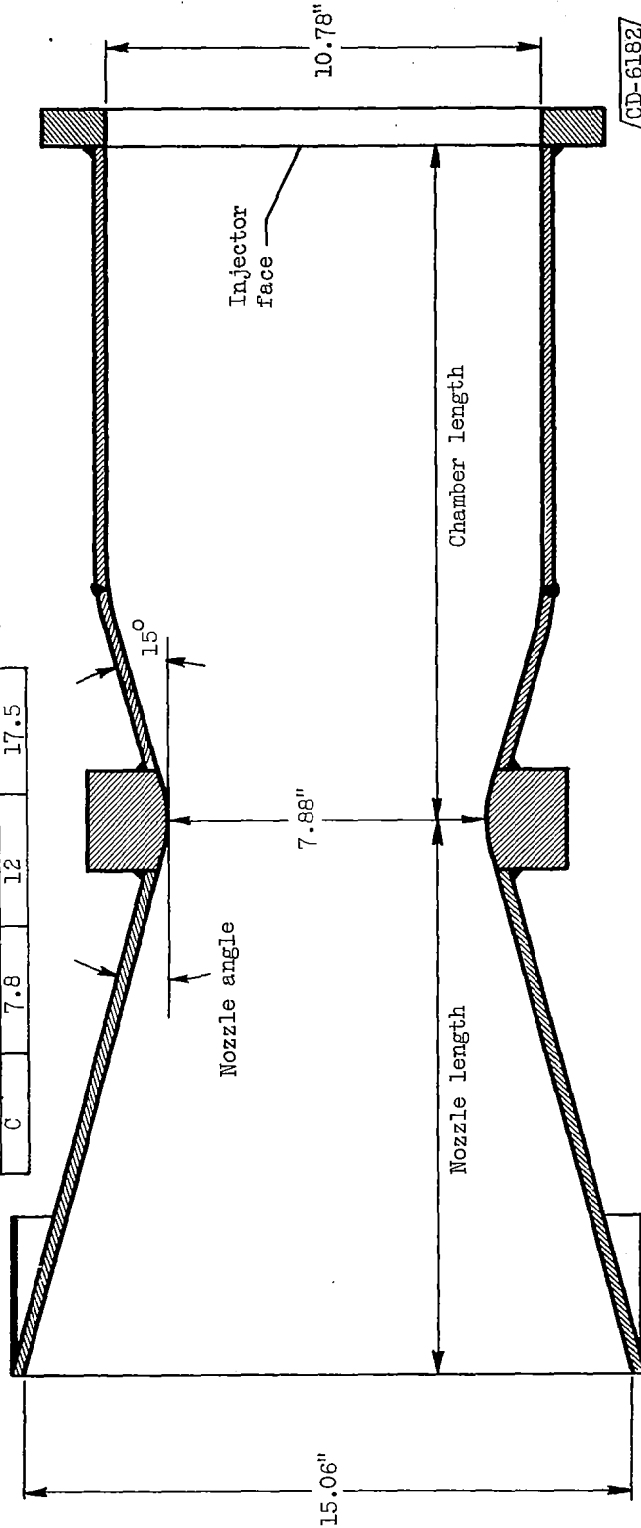
Figure 5. - Uncooled rocket thrust chamber for 20,000-pound thrust, chamber pressure of 300 pounds per square inch absolute, and sea-level expansion.

Fuel

Oxidant
tube

Injector
face

Distribution
plate

Fuel

Oxidant

Fuel
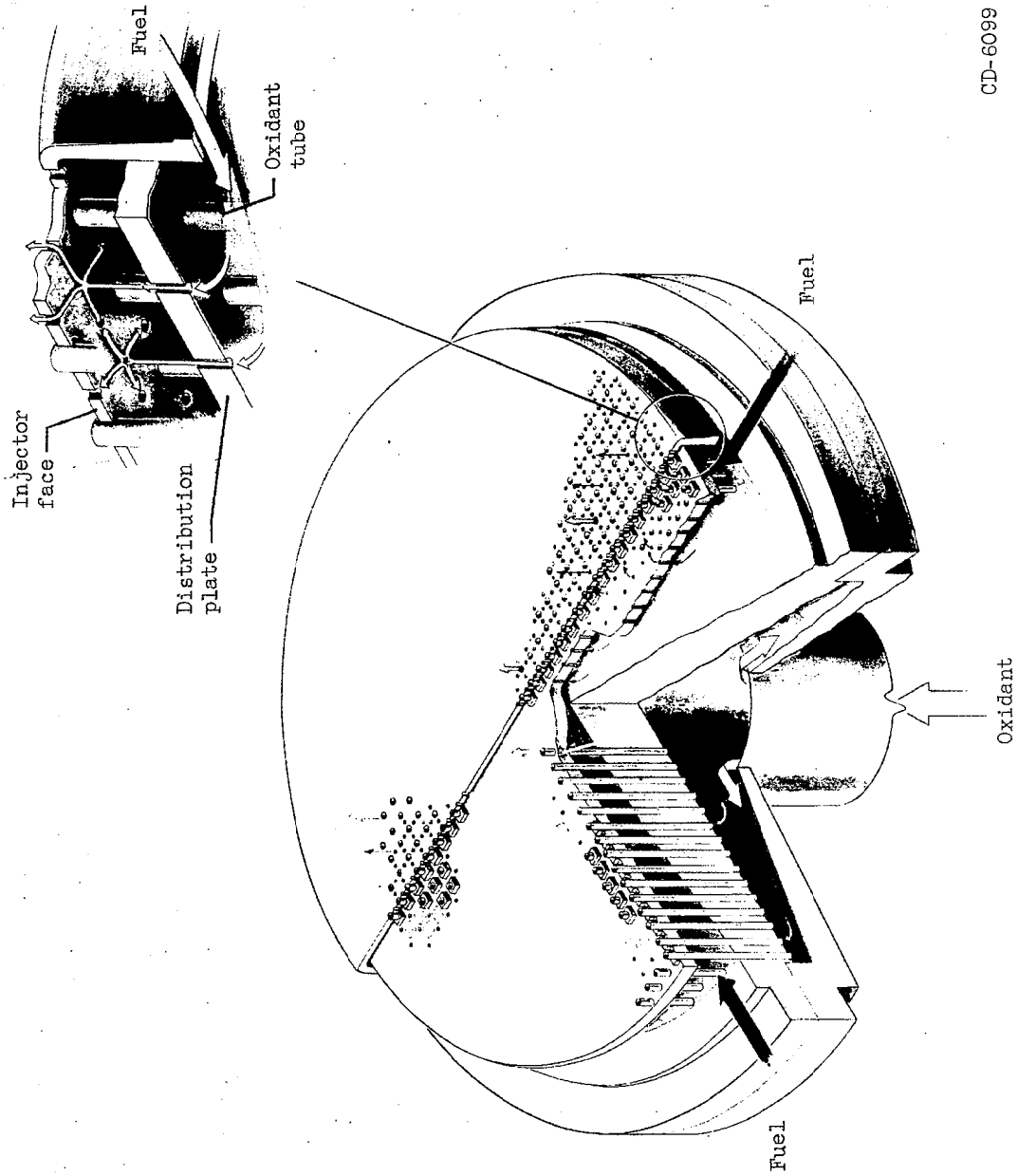
CD-6099

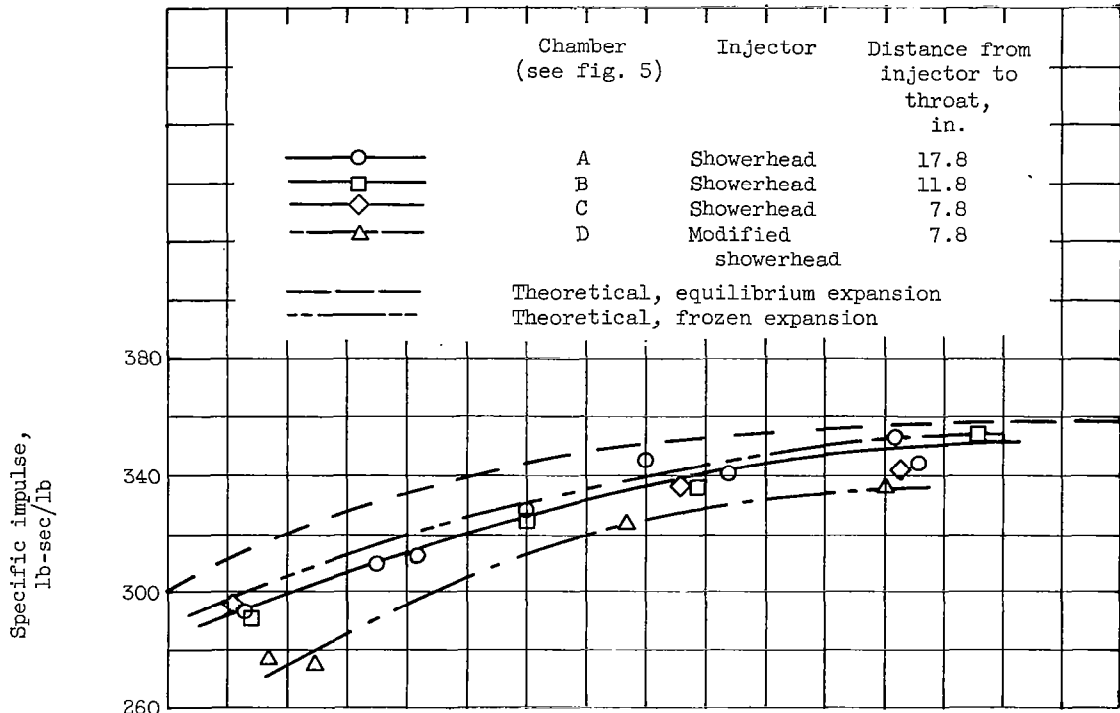Figure 6. - Cutaway view of 20,000-pound-thrust injector showing propellant distribution.
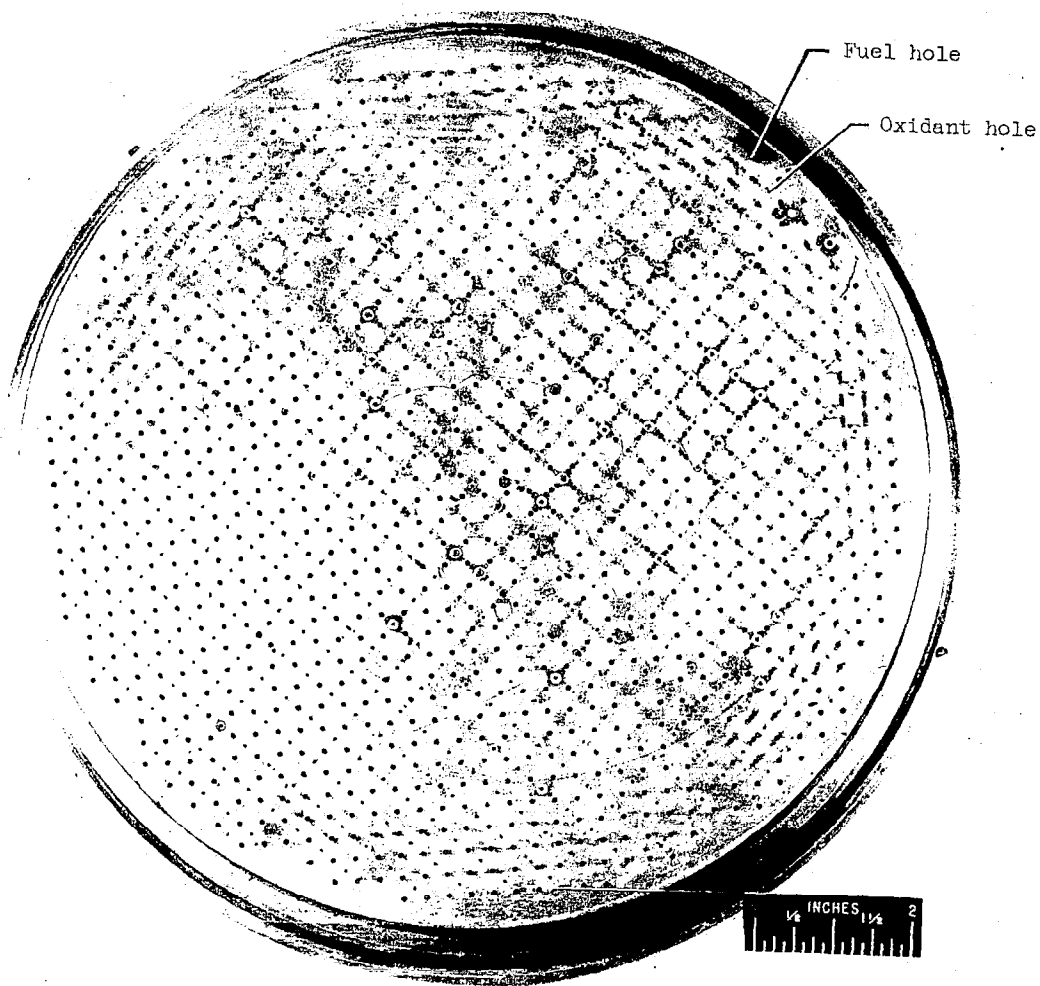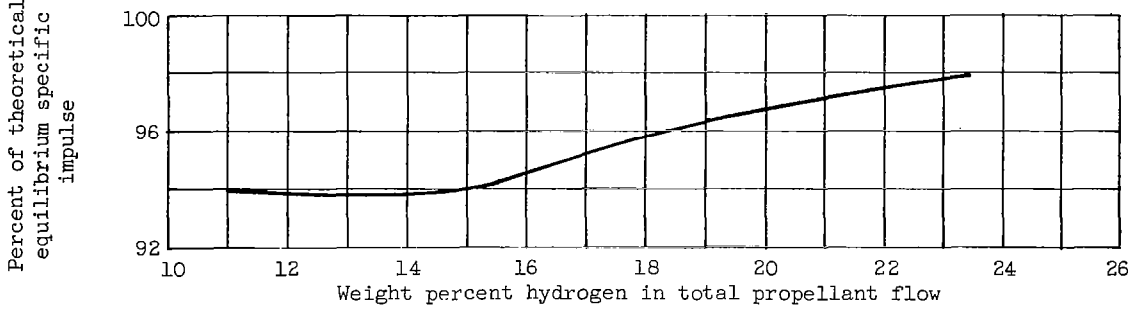
Figure 7. - Showerhead injector for 20,000-pound-thrust rocket engine.

C-47942

(a) Specific impulse.

(b) Ratio of theoretical to experimental specific impulse.

Figure 8. - Theoretical and experimental specific impulse of gaseous hydrogen and liquid oxygen in 20,000-pound-thrust rocket engine. Chamber pressure, 300 pounds per square inch absolute; sea-level expansion.
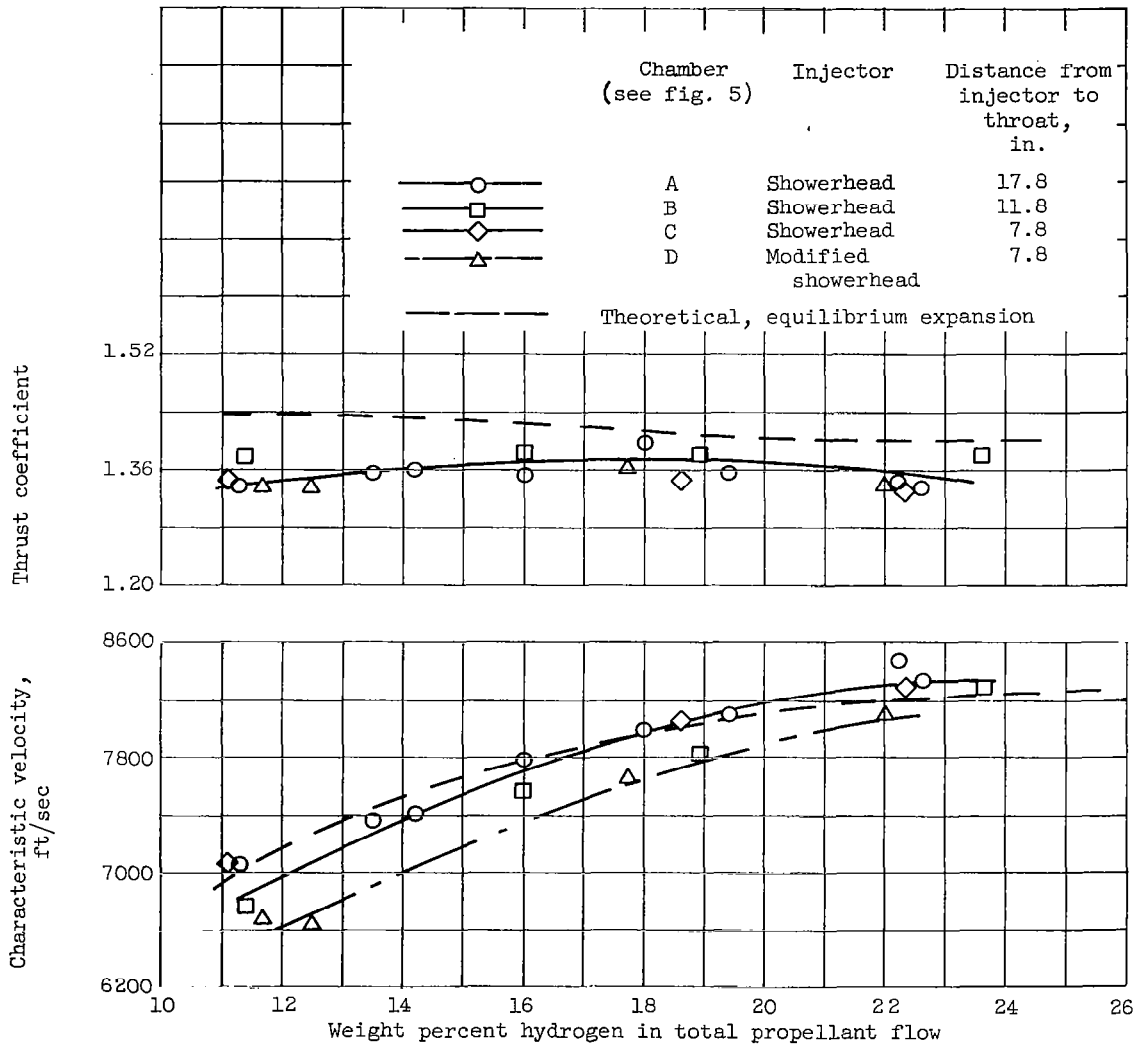
Figure 9. - Thrust coefficient and characteristic velocity of gaseous hydrogen and liquid oxygen in 20,000-pound-thrust rocket engine. Chamber pressure, 300 pounds per square inch absolute.

C-47506

Run with showerhead injector          Run with modified showerhead injector

Figure 10. - Effect of injector modification on short thrust chamber.